APRIL 02 2021

Comparison of mesopelagic organism abundance estimates using *in situ* target strength measurements and echo-counting techniques ⓔⓟ

Emma Cotter; Christopher Bassett; Andone Lavery

Check for updates

CrossMark

View Online

Export Citation

Comparison of mesopelagic organism abundance estimates using *in situ* target strength measurements and echo-counting techniques (EP)

Emma Cotter,[1,a)] Christopher Bassett,[2,b)] and Andone Lavery[1,c)]

[1]*Department of Applied Ocean Physics and Engineering, Woods Hole Oceanographic Institution, Woods Hole, Massachusetts 02543, USA*
[2]*Applied Physics Laboratory, University of Washington, Seattle, Washington 98105, USA*

ecotter@whoi.edu, cbassett@uw.edu, alavery@whoi.edu

Abstract: Recent studies using acoustic techniques suggest that the biomass of mesopelagic fishes may be an order of magnitude higher than previously estimated from trawls. However, there is uncertainty surrounding these estimates, which are derived from shipboard echosounder measurements using necessary, but poorly constrained, assumptions. Here, an echosounder is used to measure individual target strengths at depth. These measurements are used to infer mesopelagic organism density through echo-counting. Measured target strengths are used to estimate organism density by inverting shipboard echosounder measurements. The two sampling methods agree well, but highlight the importance of accurate target strength measurements. © 2021 Author(s). All article content, except where otherwise noted, is licensed under a Creative Commons Attribution (CC BY) license (http://creativecommons.org/licenses/by/4.0/).

The mesopelagic zone of the ocean ($\approx$200–1000 m deep) is home to a diverse community of small fishes and other organisms. Recent estimates of global mesopelagic fish biomass are as high as 15 Gt, but estimates span an order of magnitude (1–15 Gt).[1,2] These estimates, in conjunction with increasing global population and depletion of fish stocks, have spurred interest in the development of commercial mesopelagic fisheries.[3] However, mesopelagic species are a critical part of the food web, and their diel migration plays a major role in the ocean carbon cycle.[4] Sustainable development would therefore require improved biomass estimates and a better understanding of animal distributions, behavior, and life history.

Quantification of mesopelagic biomass is not straightforward: net trawls can provide insight into species distribution, but may undersample relative abundance due to avoidance and net selectivity.[5] Active acoustic measurements can circumvent this issue by sampling remotely, but interpretation of acoustic data comes with its own set of challenges. Typically, volume backscatter is measured using shipboard echosounders. At the ranges of interest, large sampling volumes typically preclude detection of individual targets. Therefore, conversion of shipboard measurements to biomass requires several assumptions. First, representative groups of organisms must be selected (e.g., grouped by species, size), and an assumption must be made about their relative abundance. Second, the acoustic target strength (*TS*), at the measurement frequency for each group must be assumed or measured. Finally, to convert density to biomass, the mass of individual organisms must be assumed or measured and related to *TS* using time- and labor-intensive trawls.

This approach has been used extensively for epipelagic fisheries applications: net trawls are used to determine the species present and their size distributions, and length-*TS* relationships for those species are used to determine the appropriate target strength values for inversion of shipboard measurements to abundance. Data are commonly collected at 38 kHz, a frequency that, for most epipelagic fishes, falls in the geometric scattering regime where acoustic backscatter is relatively insensitive to frequency.[6]

Application of the same methods in the mesopelagic is more complicated for several reasons. First, 38 kHz is near the resonant frequencies of many gas-bearing mesopelagic organisms, making measurements sensitive to the nonlinear scattering response.[7,8] Second, the target strengths of gas-bearing organisms may change with depth[7,9] so *TS* measurements performed near the surface or in tanks may not be accurate when the same organisms are observed at depth. Despite these complicating factors, several estimates of mesopelagic biomass rely on data collected by shipboard

[a)]Author to whom correspondence should be addressed, ORCID: 0000-0001-9162-9063.
[b)]ORCID: 0000-0003-0534-0664.
[c)]ORCID: 0000-0002-0713-1623.

echosounders operating at 38 kHz.[1,2,10–12] These estimates use a combination of *TS* measurements made at or near the surface and resonance models with parameters based on trawl data.

In situ measurements of *TS* and organism density can help to reduce the uncertainty surrounding these estimates. Several recent studies have deployed 38 kHz echosounders within the mesopelagic zone.[13–16] Notably, in the Tasman Sea, Kloser *et al.*[13] found that estimated volume backscatter from *in situ* measurements of *TS* and organism density agreed well with shipboard echosounder data. However, Kloser *et al.*[13] did not perform echo-integration to explore the importance of accurate *TS* values on estimates of organism density.

Our recent work[8,17] has analyzed broadband, *in situ TS* measurements of mesopelagic organisms in a frequency band that contains 38 kHz (25–40 kHz). We observed organisms at or near-resonance at 38 kHz, as well as organisms with resonance frequencies above 38 kHz (i.e., *TS* is increasing with frequency at 38 kHz), indicating that *TS*-length relationships at this frequency will not be sufficient for estimations of mesopelagic organism abundance. Here, we compare estimates of organism abundance from echo-counting of targets at short ranges to estimates achieved by applying echo-integration using *in situ* measurements of target strength and volume backscattering measured by a concurrently operating shipboard echosounder.

1. Methods

1.1 Instrumentation platform

In situ measurements were made using Deep-See, a cabled, towed instrumentation platform that includes a custom Airmar transducer with a nominal frequency range of 18–45 kHz. This transducer is operated by a custom bistatic Edgetech system with an eight-sector polyvinylidene floride (PVDF) array as a receiver. Details of this system can be found in Bassett *et al.*[8] and Cotter *et al.*[17] An onboard Seabird 25+ conductivity, temperature, and depth (CTD) sensor is used to measure water properties and platform depth.

The Airmar transducer transmitted a linear frequency modulated chirp (18.5–47.5 kHz) with a pulse duration of 10 ms at a ping rate of 0.5 Hz. Data were collected to a range of 300 m. The system gain, $G(f)$, was calculated *in situ* using a combination of full- and partial-wave techniques,[8,18,19] and the beampattern of the bistatic system, $b(f, \phi)$, where ϕ is the off-axis angle, was evaluated in a test well.[17]

1.2 Data collection

Data were collected during a 24 July–7 August 2019 cruise on the R/V Bigelow off of the New England continental shelf break (near 39°20″ N, 69°24″ W, water depth between 2000 and 3000 m). This work focuses on three deployments of Deep-See that were conducted on 27 July, 1 August, and 4 August 2019, referred to as D1, D2, and D3, respectively. Analysis is limited to data collected between 200 and 800 m depth during daytime hours (8:00 to 16:00 local time) to avoid diel migration. Concurrent measurements of volume backscattering (S_v) were made with a shipboard narrowband Simrad EK60 system operating at 18, 38, 120, and 200 kHz (only the 38 kHz channel is analyzed here). The EK60 was calibrated on 20 August 2019, and data have been corrected for the low-power non-linearity.[20] Power values below −130 dB re 1 W use the same correction due to limited measurements in this range. EK60 data were processed using the Echolab MATLAB library.[21] Due to drag, Deep-See lagged behind the surface vessel, and shipboard measurements are not exactly co-temporal/co-spatial. The vessel GPS tracks, 38 kHz shipboard echosounder data, and Deep-See depth profile for each deployment are shown in Figs. S1 and S2 in the supplemental material.[22] During deployments, vessel speed was approximately two knots, and midwater trawling (using a similar net as in De Robertis *et al.*[23]) was performed in conjunction with Deep-See deployments. Detailed analysis of these trawls is beyond the scope of this paper.

1.3 Processing of in situ data

Matched-filtering and split-beam processing. Matched-filtering[24] was performed in the Edgetech data acquisition software before recording the filtered, decimated analytic signal for each of the eight channels of the PVDF array. We only use the matched-filter output for the inner four sectors of the array, whose geometry resembles four-sector split-beam transducers. The coherent sum of the matched-filtered signal from these four quadrants is referred to as *v*. Split-beam processing was used to determine the alongship and athwartship angles, ϕ_f and ϕ_p, respectively, and the broadband off-axis angle, ϕ, was calculated as $\sqrt{\phi_f^2 + \phi_p^2}$. A general description of split-beam processing can be found in Simmonds *et al.*,[6] and a description of the implementation for this system can be found in Bassett *et al.*[8]

Target processing. The minimum range for target detection (r_{min}) was 10 m to avoid bistatic effects from the transducer/receiver array, while the maximum range for target detection (r_{max}) was adjusted ping-by-ping to restrict target detection to regions where individual targets were detectable using the echogram (broadband *TS*). The echogram was divided into 20-s, 2-m bins, and the median value was calculated for each bin. Individual targets were considered detectable in bins where the median did not exceed −85 dB re 1 m^2 (Fig. S3).[22] This threshold was tuned empirically, though agreement between organism density estimates provides validation. Targets were then detected in the region between r_{min} and r_{max} following the Echoview single target detection algorithm, as in Cotter *et al.*[17]

For each detected target, target strength as a function of frequency, $TS(f)$, was calculated using an 0.3 m window centered around the target peak, v_{targ}. First, a Tukey window with a cosine fraction of 0.05 was applied to v_{targ}. The signal v_{targ} was zero-padded to a length of 2048 points before calculating a fast Fourier transform (FFT). The target strength spectrum, in dB re 1 m^2, was then calculated as

$$TS(f) = 20\log_{10}(|V_{targ}|) + 40\log_{10}(r_{pk}) + 2\alpha(f)r_{pk} + 2G(f) + b(\phi, f), \tag{1}$$

for $25 \leq f \leq 40$ kHz, where r_{pk} is the range to the peak in v, and $\alpha(f)$ is the attenuation coefficient.[25]

The system noise floor, NF, was estimated using data collected by deploying the transducer/receiver array in the same manner as it was for data collection, but operating in passive mode. The noise spectra were calculated in 0.5 m bins between 15 and 200 m range for 104 pings collected in passive mode as $NF(f) = 20\log_{10}(|V|)$, where V is the power spectrum of the 0.5 m window, calculated using the FFT. The mean noise spectrum for each range bin was calculated. The resulting curves were relatively flat and no range dependence was observed. The noise floor for the transducer was then calculated as the linear mean across all ranges, and the minimum detectable target strength as a function of frequency and range, $TS_{min}(f, r)$, was $NF(f) + 40\log_{10}(r)$. Attenuation is neglected due to the relatively low frequencies and short ranges of interest. Any targets for which $TS(f)$ did not exceed TS_{min} by at least 10 dB re 1 m^2 for more than 80% of the frequency band were rejected. This threshold was selected to avoid rejection of targets with nulls that fell below the noise floor. Targets were then tracked through the beam using the ECHOVIEW alpha-beta tracking algorithm implemented in MATLAB 2019b. Target detection and tracking parameters are the same as in Cotter *et al.*[17]

Target strength at 38 kHz. A representative narrowband target strength at 38 kHz, TS_{38}, was calculated for each target as the linear average of $TS(f)$ from 37–39 kHz. If a target was detected multiple times, $TS(f)$ for the target was defined as the linear average of $TS(f)$ for all detections. The average target strength as a function of depth, $\overline{TS_{38}}(z)$, was calculated for all targets from each deployment in 25 m depth bins.

1.4 Organism density from echo-counting

Individual target detection data were used to estimate organism density as a function of depth and TS_{38} (echo-counting[6]) To do this, the volume of water sampled, $V_s(z)$, was calculated in 25 m depth bins. The volume of water sampled by each ping was approximated by a cone of volume $V_s = (\pi/3)(r_2^3 - r_1^3)\tan(\phi_{max})$, where $\phi_{max} = 2°$ is the maximum off-axis angle for target detection, and r_2 and r_1 are the maximum and minimum ranges sampled within the depth bin, respectively, and may be defined by the edge of the depth bin or by r_{min}/r_{max} (as illustrated in Fig. S4).[22] Organism density as a function of depth and TS_{38} estimated by echo-counting (ec) was calculated in 25 m depth and 2 dB TS_{38} bins:

$$\rho_{ec}(z, TS_{38}) = \frac{n(z, TS_{38})}{V_s(z)}, \tag{2}$$

where $n(z, TS_{38})$ is the number of targets detected in each depth/target strength bin. The total organism density in each depth bin estimated by echo-counting was calculated as

$$\rho_{ec}(z) = \frac{n(z)}{V_s(z)}, \tag{3}$$

where $n(z)$ is the number of targets detected in each depth bin.

1.5 Organism density from volume backscattering

The volume backscattering coefficient, s_v, in m^{-1} ($S_v = 10\log_{10}s_v$), can be related to organism density by $s_v = \sum_{k=1}^{K}\rho_k\sigma_{bs,k}$, where ρ_k is the volumetric density of organisms with backscattering cross section $\sigma_{bs,k}$, in m^2 ($TS = 10\log_{10}\sigma_{bs}$), and there are K different groups of organisms present. At a given point within the beam, this is equivalent to $s_v = \rho\overline{\sigma_{bs}}$ where ρ is the density of all organisms within the beam, and $\overline{\sigma_{bs}}$ is the average volume backscattering cross section of all organisms within the beam. Therefore, we can use depth-dependent (dd) *in situ TS* measurements to approximate organism density from volume backscatter at 38 kHz (echo-integration[6]),

$$\rho_{sv,dd}(z) = 10^{\left[S_v - \overline{TS_{38}}(z)\right]/10}. \tag{4}$$

For comparison, organism density was also estimated using the water column mean $\overline{TS_{38}}$. This estimate will be referred to as $\rho_{sv,wc}$.

Because the intensity, and possibly the composition, of layers changed with time, organism density was calculated using S_v in the region sampled by Deep-See rather than an average value for the entire deployment. For each Deep-See ping, a one-minute average of s_v measured by the shipboard echosounder (temporally centered on the timestamp of the Deep-See ping) was calculated in the range between r_{min} and r_{max}. Local s_v measurements were then averaged in 25 m depth bins for each deployment based on the average sampled depth for each ping. These values will be referred to as the
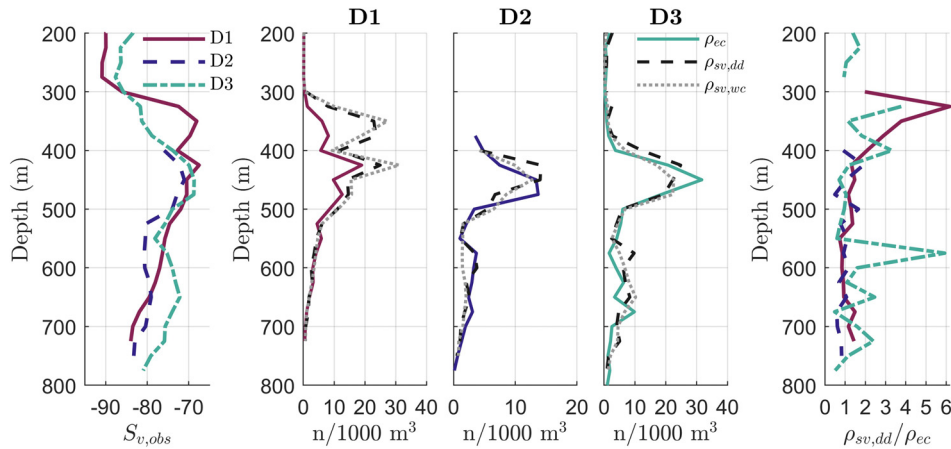
Fig. 1. Left: Shipboard volume backscatter in the region sampled by the *in situ* echosounder ($S_{v,obs}$) for each deployment. Center: Comparison of three organism density estimates for each deployment. The coloured line indicates ρ_{ec}, organism density estimated by echo-counting using *in situ* data. The black, dashed line indicates $\overline{TS_{38}}(z)$ to $S_{v,obs}$. The gray, dotted line indicates $\rho_{sv,wc}$, the organism density estimated using the water column mean target strength for each deployment, $\overline{TS_{38}}$. Note that the scale of the x axes varies between deployments to highlight differences between density estimates. Right: The ratio of the estimates by echo-integration ($\rho_{sv,dd}$) to echo-counting (ρ_{ec}) for each deployment.

observed volume backscatter, $S_{v,obs}$. While the lag of Deep-See behind the vessel is unknown, and therefore not accounted for, inclusion of an estimation of lag did not substantially change our results.

2. Results

While the three deployments sites were geographically similar, notable differences in the shape and magnitude of $S_{v,obs}$ and estimates of organism density are observed (Fig. 1). Two distinct scattering layers (peaks in $S_{v,obs}$) are observed in D3 with peaks around 450 and 650 m, while just one layer at 450 m is observed in D2 (no daytime Deep-See data were collected above ~400 m, but no second layer is observed in the shipboard echosounder data). A relatively intense scattering layer ($S_v \approx -65$ dB re 1/m) was observed in D1 between 300 and 400 m, and inspection of the shipboard echograms (Fig. S2)[22] shows that this scattering layer moved lower in the water column later in the day (this may be due to temporal changes in biomass distribution or spatial changes in vessel position). Figure S5 shows the number of targets detected in each depth bin for each deployment.[22] Of these targets, 82% were at least 15 dB above the noise floor over the entire the frequency band. Fish (predominately stomiiformes and myctophids) dominated midwater trawls by number, though various gelatinous organisms contributed a significant fraction of sampled biomass.

While the water column mean $\overline{TS_{38}}$ did not vary significantly between deployments ($\overline{TS_{38}} = -52.4, -52.1$, and -52.3 dB for D1–D3, respectively), differences in the trends in $\overline{TS_{38}}(z)$ with depth were observed (Fig. 2). $\overline{TS_{38}}(z)$ was relatively constant with depth for D1. More complex profiles of $\overline{TS_{38}}(z)$ were observed for D2 and D3. In D2, a distinct trough is observed in $\overline{TS_{38}}(z)$ around 600 m depth ($\overline{TS_{38}} = -56$ dB re 1 m^2 between 575 and 600 m). The density of weakly scattering organisms (low TS_{38}) at this depth is similar to that observed within the scattering layer, but fewer strongly
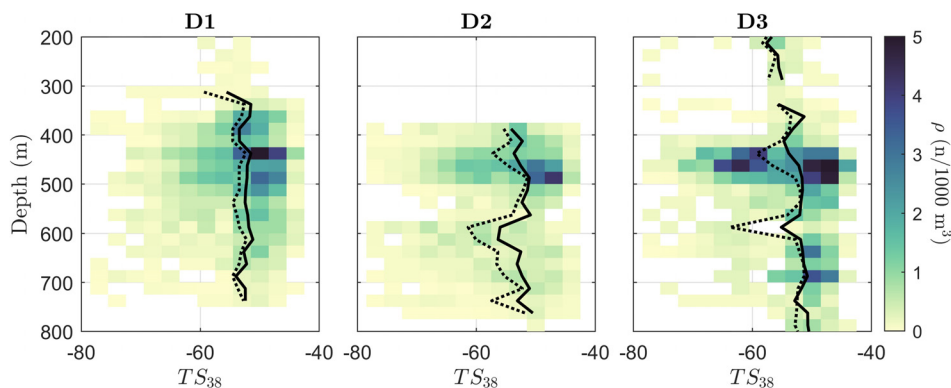

Fig. 2. $\rho(z, TS_{38})$ for each deployment. The solid black line indicates $\overline{TS_{38}}(z)$, the average target strength at each depth, in dB re 1 m^2, and the dotted line shows the median. White indicates TS/depth bins where no data were collected.

scattering organisms (high TS_{38}) are present, resulting in a lower mean value. In D3, there is a general increase in TS_{38} with depth, and there is a higher density of organisms with TS below -60 dB within the scattering layer than is observed in D1 or D2. Increasing TS_{38} can result from swimbladder compression with increasing pressure, but the more complex trends observed indicate that changing species compositions with depth also play a role.

For D1, the estimates of organism density using the shipboard data ($\rho_{sv,dd}$ and $\rho_{sv,wc}$) exceed the estimate from echo-counting (ρ_{ec}) by up to a factor of 6 between 300 and 400 m (Fig. 1). This may be attributed to the limited number of individual targets detected in this region due to high target densities, resulting in a small sample size (Fig. S6).[22] The three estimates of organism density agree well lower in the water column, and there is little deviation between $\rho_{sv,dd}$ and $\rho_{sv,wc}$ due to limited variation in $\overline{TS_{38}}(z)$ with depth. For D2, ρ_{ec} and $\rho_{sv,dd}$ agree relatively well throughout the water column. However, $\rho_{sv,wc}$ underestimates organism density around 600 m depth because the lower $\overline{TS_{38}}$ in this region is not represented by the water column average. The three estimates again agree relatively well for D3, especially within the scattering layer between 400 and 500 m depth. However, the estimate from echo-counting underestimates echo-integration at some points below 500 m depth, which may be due to limited data collected in this region (Fig. S2).[22] We note that agreement between ρ_{ec} and $\rho_{sv,dd}$ improved when accounting for the EK60 non-linearity, which can lead to overestimates of abundance from low-power received signals.[20]

3. Discussion and conclusions

We have presented *in situ* measurements of mesopelagic organism density and compared them with estimates derived from volume backscatter measured by a shipboard echosounder without any assumptions about species composition. In general, the estimates agree well, indicating that when representative target strength values are used, accurate estimates of mesopelagic organism abundance can be achieved from ship-based measurements. We do not attempt to translate these measurements to an estimate of biomass, because such estimates require information regarding species composition and size distributions.

The differences between the three methods employed to estimate organism abundance beg the question "how should organism density be measured?" Echo-counting (ρ_{ec}) is likely the most accurate method, but is not a scalable solution and fails in the highest density regions. Given these limitations, estimates applying depth-dependent target strength measurements ($\rho_{sv,dd}$) to shipboard data,[6] are likely the most feasible to implement at large-scale. Differences between $\overline{TS_{38}}(z)$ with depth and between deployments highlight the importance of accurate, depth-dependent target strength values for estimations of organism abundance. Notable shifts in depth-dependent TS measurements may also provide insight into changing species compositions. Accurate biomass estimates will require a better understanding of species distribution in the mesopelagic and further *in situ* measurements of target strength at different frequencies.

The TS_{38} values measured *in situ* using Deep-See are higher than those used for existing global biomass estimates derived from shipboard acoustic data at 38 kHz. We do not argue that our measurements alone should be used for global studies, but make this comparison to relate our measurements to global biomass estimates. However, we note similarities between our measurements of mesopelagic TS_{38} and those made in the Tasman Sea (mean TS_{38} between -55.4 and -50.3 dB re 1 m^2)[13] and the Red Sea (mean $TS_{38} \approx -55$ dB re 1 m^2).[5] Irigoien *et al.*[1] used $TS_{38} = -60.6$ dB re 1 m^2, a geometric average of TS_{38} values in the literature, to generate a global biomass estimate. This value is significantly lower than the TS_{38} values presented here, and, when used in lieu of $\overline{TS_{38}}$ to calculate $\rho_{sv,wc}$ at our test site, results in estimates of organism density as much as $10\times$ higher than would the TS estimates presented in this paper. These differences in TS_{38} can be attributed, in part, to the fact that Irigoien *et al.*[1] use a geometric average of TS values rather than a linear average. Proud *et al.*[2] assumed that all mesopelagic volume backscatter was contributed by gas-bearing organisms, and modeled three scenarios: (1) all fish have gas-filled swimbladders, (2) all fish have swimbladders, but some lose them with age, and (3) some fish have swimbladders. Median TS_{38} values from each model scenario were used to generate global biomass estimates. Our TS_{38} measurements (median TS_{38} of -53.7, -53.9, and -53.7 for D1–D3, respectively) are closest to scenario 1, which had a median value of -53.8 dB re 1 m^2. However, we note that the median value does not carry physical significance in this application: it may provide a statistical description of the TS distribution in a population, but the only statistic suitable for echo-integration is the linear average.[26]

References and links

[1] X. Irigoien, T. Klevjer, A. Røstad, U. Martinez, G. Boyra, J. Acuña, A. Bode, F. Echevarria, J. Gonzalez-Gordillo, S. Hernandez-Leon, S. Agusti, D. L. Aksnes, C. Duarte, and S. Kaartvedt, "Large mesopelagic fishes biomass and trophic efficiency in the open ocean," Nat. Commun. **5**, 3271 (2014).

[2]R. Proud, N. Handegard, R. J. Kloser, M. J. Cox, and A. S. Brierley, "From siphonophores to deep scattering layers: Uncertainty ranges for the estimation of global mesopelagic fish biomass," ICES J. Mar. Sci. **76**(3), 718–733 (2019).

[3]W. Sutherland, S. Broad, S. Butchart, S. Clarke, A. Collins, L. Dicks, H. Doran, N. Esmail, E. Fleishman, N. Frost, K. Gaston, D. Gibbons, A. Hughes, Z. Jiang, R. Kelman, B. LeAnstey, X. le Roux, F. Lickorish, K. Monk, D. Mortimer, J. Pearce-Higgins, J. Peck, J. Pettorelli, C. Seymour, M. Spalding, J. Wentworth, and N. Ockendon, "A horizon scan of emerging issues for global conservation in 2019," Trends Ecol. Evol. **34**(1), 83–94 (2019).

[4]M. Costello and S. Breyer, "Ocean depths: The mesopelagic and implications for global warming," Curr. Biol. **27**(1), R36–R38 (2017).

[5]S. Kaartvedt, A. Staby, and D. Aksnes, "Efficient trawl avoidance by mesopelagic fishes causes large underestimation of their biomass," Mar. Ecol. Prog. Ser. **456**, 1–6 (2012).

[6]E. Simmonds and D. MacLennan, *Fisheries Acoustics*, 2nd ed. (Blackwell Science, Oxford, UK, 2005).

[7]P. Davison, A. Koslow, and R. Kloser, "Acoustic biomass estimation of mesopelagic fish: Backscattering from individuals, populations, and communities," ICES J. Mar. Sci. **72**(5), 1413–1424 (2015).

[8]C. Bassett, T. K. Stanton, A. C. Lavery, and E. Cotter, "Frequency- and depth-dependent target strength measurements of individual mesopelagic scatterers," J. Acoust. Soc. Am. **148**, EL153–EL158 (2020).

[9]J. Horne, K. Sawada, K. Abe, R. Kreisberg, D. Barbee, and K. Sadayasu, "Swimbladders under pressure: Anatomical and acoustic responses by walleye pollock," ICES J. Mar. Sci. **66**(6), 1162–1168 (2009).

[10]P. Escobar-Flores, R. O'Driscoll, J. Montgomery, Y. Ladroit, and S. Jendersie, "Estimates of density of mesopelagic fish in the southern ocean derived from bulk acoustic data collected by ships of opportunity," Polar Biol. (**43**, 43–61 (2020).

[11]R. Proud, M. Cox, and A. Brierley, "Biogeography of the global ocean's mesopelagic zone," Curr. Biol. **27**(1), 113–119 (2017).

[12]T. Klevjer, X. Irigoien, A. Røstad, E. Fraile-Nuez, V. Benítez-Barrios, and S. Kaartvedt, "Large scale patterns in vertical distribution and behaviour of mesopelagic scattering layers," Sci. Rep. **6**, 1–11 (2016).

[13]R. Kloser, T. Ryan, G. Keith, and L. Gershwin, "Deep-scattering layer, gas-bladder density, and size estimates using a two-frequency acoustic and optical probe," ICES J. Mar. Sci. **73**(8), 2037–2048 (2016).

[14]K. Benoit-Bird, M. Moline, and B. Southall, "Prey in oceanic sound scattering layers organize to get a little help from their friends," Limnol. Oceanogr. **62**(6), 2788–2798 (2017).

[15]S. Kaartvedt, A. Røstad, S. Christiansen, and T. Klevjer, "Diel vertical migration and individual behavior of nekton beyond the ocean's twilight zone," Deep Sea Res. Part I: Oceanogr. Res. Papers **160**, 103280 (2020).

[16]I. Dias Bernardes, E. Ona, and H. Gjøsæter, "Study of the Arctic mesopelagic layer with vessel and profiling multifrequency acoustics," Prog. Oceanogr. **182**, 102260 (2020).

[17]E. Cotter, C. Bassett, and A. Lavery, "Classification of broadband target spectra in the mesopelagic using physics-informed machine learning," J. Acoust. Soc. Am (to be published).

[18]T. Stanton and D. Chu, "Calibration of broadband active systems using a single standard spherical target," J. Acoust. Soc. Am **124**(1), 128–136 (2008).

[19]T. Stanton, D. Chu, J. Jech, and J. Irish, "New broadband methods for resonance classification and high-resolution imagery of fish with swimbladders using a modified commercial broadband echosounder," ICES J. Mar. Sci. **67**, 365–378 (2010).

[20]A. De Robertis, C. Bassett, L. N. Andersen, I. Wangen, S. Furnish, M. Levine, and P. Ratilal, "Amplifier linearity accounts for discrepancies in echo-integration measurements from two widely used echosounders," ICES J. Mar. Sci. **76**(6), 1882–1892 (2019).

[21]R. Towler, "EchoLab MATLAB based EK60 Library," software package (2017), https://bitbucket.org/afsc_mace/matlab-echolab/src/master (Last viewed 12/15/2020).

[22]See supplementary material at https://www.scitation.org/doi/suppl/10.1121/10.0003940 for supplemental figures.

[23]A. De Robertis, K. Taylor, K. Williams, and C. Wilson, "Species and size selectivity of two midwater trawls used in an acoustic survey of the Alaska arctic," Deep-Sea Res. II (**135**), 40–50 (2017).

[24]D. Chu and T. Stanton, "Application of pulse compression techniques to broadband acoustic scattering by live individual zooplankton," J. Acoust. Soc. Am. **104**(1), 39–55 (1998).

[25]R. E. Francois and G. R. Garrison, "Sound absorption based on ocean measurements. Part II: Boric acid contribution and equation for total absorption," J. Acoust. Soc. Am. **72**(6), 1879–1890 (1982).

[26]K. Foote, "Linearity of fisheries acoustics, with addition theorems," J. Acoust. Soc. Am. **73**(6), 1932–1940 (1983).